

Entropy production in classical Yang-Mills theory from Glasma initial conditions

Hideaki Iida,¹ Teiji Kunihiro,¹ Berndt Müller,² Akira Ohnishi,³ Andreas Schäfer,^{4,3} and Toru T. Takahashi⁵

¹*Department of Physics, Kyoto University, Kyoto 606-8502, Japan*

²*Department of Physics & CTMS, Duke University, Durham, NC 27708, USA*

³*Yukawa Institute for Theoretical Physics, Kyoto University, Kyoto 606-8502, Japan*

⁴*Institut für Theoretische Physik, Universität Regensburg, D-93040 Regensburg, Germany*

⁵*Gumma National College of Technology, Gumma 371-8530, Japan*

(Dated: February 25, 2022)

We study the thermalization process in classical Yang-Mills (CYM) field theory starting from noisy glasma-like initial conditions by investigating the initial-value sensitivity of trajectories. Kunihiro *et al.* [17] linked entropy generation to the Kolmogorov-Sinai entropy, which gives the entropy production rate in classical chaotic systems, calculated numerically for CYM fields starting from purely random initial field configurations. In contrast, we here study glasma-like initial conditions. For small random fluctuations we obtain qualitatively similar results while no entropy increase is observed when such fluctuations are absent. We analyze the intermediate time Lyapunov spectrum for several time windows and calculate the Kolmogorov-Sinai entropy. We find a large number of positive Lyapunov exponents at the early stages of time evolution. Also for later times their number is a sizeable fraction of the total number of degrees of freedom. The spectrum of positive Lyapunov exponents at first changes rapidly, but then stabilizes, indicating that the dynamics of the gauge fields approaches a steady state. Thus we conclude that also for glasma-like initial conditions a significant amount of entropy is produced by classical gluon field dynamics.

I. INTRODUCTION

A. Motivation

Elucidating the mechanism of entropy production and early thermalization leading to quark-gluon plasma (QGP) formation is one of the fundamental problems posed by the phenomenological analyses of the experimental data obtained from the Relativistic Heavy-Ion Collider (RHIC) at Brookhaven National Laboratory and the Large Hadron Collider (LHC) at CERN. As hydrodynamics is only applicable after local thermalization has occurred, massive entropy production is a basic ingredient for any detailed understanding of the time-evolution of heavy-ion collisions. Analyses based on ideal relativistic hydrodynamic equations suggest that thermalization should be achieved in an early stage in order to explain the RHIC data. The thermalization time is estimated to be $\tau_0 \simeq 1$ fm/c [1, 2], which is significantly shorter than the equilibration time obtained in perturbative QCD [3]. If τ_0 were much longer, one would have to expect that significant artifacts caused by incomplete thermalization could affect many interpretations of the experimental data.

The “early thermalization” of the created matter should be explained on the basis of the underlying dynamics of the time-evolution of the matter created in the nuclear collision. This remains a major challenge of relativistic heavy ion physics. Apart from the time-evolution dynamics, peculiar fluctuations in the *initial conditions* are also recognized to be an important ingredient for understanding the hydrodynamic evolution of the quark gluon matter, in particular, the elliptic and triangular flows [4–7].

B. Classical Yang-Mills Fields

Classical Yang-Mills (CYM) field theory is a good starting point for describing the initial stage dynamics of relativistic heavy-ion collisions. At high energies, we excite partons with small Bjorken x and the number of gluons in the small x region is so high that they may be treated as a coherent or classical field [8, 9]. A classical solution of gluon fields in this regime is known: A nucleus at high energy can be regarded as a collection of large- x particles, the valence partons, which act as color sources that give rise to strong, transversely polarized chromo-magnetic and -electric fields. This configuration of the gluon fields is referred to as the color glass condensate (CGC). When two nuclei collide, their gluon fields interact and produce new, longitudinally polarized fields that extend between the color sources in the direction of the beam axis. This *glasma* field configuration is used as a standard initial condition for the time evolution of the matter created in relativistic heavy-ion collisions.

It is generally expected that some field instabilities could cause early thermalization; such instabilities include the Weibel instability [10, 11] and Nielsen-Olesen instability [12–14]. In both cases, the instability gives rise to an exponential growth of the amplitude of unstable modes having high energy, which are expected to cascade into a large number of modes or particles with small energies due to the nonlinear coupling of fields, until the fields are thermalized.

There are two facets in thermalization of CYM. The first aspect is the isotropization of the energy momentum tensor. The approximate isotropization is the minimal condition to apply hydrodynamics, and has been discussed in the literature [15, 16]. The second is the equilibration of the spectrum toward the Bose-Einstein

and the Fermi-Dirac distribution of gluons and quarks, respectively. While the spectrum equilibration provides for a more rigorous definition of thermalization, it has not been discussed seriously so far in CYM. One reason for this may be that classical field theories do not generally exhibit the correct equilibrium spectrum by themselves. When equipartition of energy is realized in classical equilibrium, high momentum components are favored compared with the quantum equilibrium, i.e. the Bose distribution. In the thermalization scenario described in the previous paragraph, we expect the produced particles to show quantum equilibrium spectra. Thus the very thermalization mechanism is attributed to this conversion process but it is a difficult and unsolved problem to describe non-equilibrium and non-uniform situations in terms of nonlinear classical or quantum dynamics.

C. Entropy Production

A central task to reach an understanding of early thermalization is to identify the mechanism of entropy production, which has been scarcely touched upon so far in the literature. It is to be noted that the high occupation probability of the unstable modes makes possible a quasi-classical treatment of the thermalization process in the initial stage. Furthermore, Kunihiro, Müller, Ohnishi, and Schäfer [17] noticed that the use of the Husimi-Wehrl entropy S_{HW} , the Wehrl entropy [18] defined in terms of a smeared Wigner function (the Husimi function) [19], is meaningful in the quasi-classical regime and showed that S_{HW} grows at the rate of the Kolmogorov-Sinai (KS) entropy S_{KS} in the long-time limit. The fundamental origin of entropy growth induced by the Husimi transformation is that even without an actual measurement the quantum mechanical uncertainty principle implies a minimum of coarse-graining. In other words: Information which cannot be measured in accordance with the uncertainty principle is de facto lost and information loss is equivalent to entropy growth.

Here the KS entropy is defined as a sum of the positive Lyapunov exponents λ_i ,

$$S_{\text{KS}} = \sum_{i, \lambda_i > 0} \lambda_i. \quad (1)$$

The size of a Lyapunov exponent λ_i is an indicator for the initial-value sensitivity of trajectories defined through the equation, $|\delta X_i(t)| \simeq |\delta X_i(t_0)| \exp[\lambda_i(t - t_0)]$, where δX_i represents a small difference of phase-space variables at the initial time $t = t_0$. A positive Lyapunov exponent means that the distance between the two phase space points grows exponentially in time. Thus the entropy production in classical dynamics is closely related to the chaoticity of the system. It is therefore quite pertinent to investigate possible entropy production of the classical field itself to study the thermalization mechanism through its chaotic behavior in the glasma stage.

In fact, the study of the chaotic properties of the classical evolution of Yang-Mills fields has a long history [20], initiated by the observation of chaotic behavior in the infrared limit of Yang-Mills theories [21], which was confirmed later for the compact lattice formalism of classical Yang-Mills theory [22]. Some properties of Lyapunov exponent and KS entropy in compact lattice gauge theories are discussed in [23] and [24], respectively.

In Ref. [25], the authors analyzed the exponential growth of the distance between two trajectories for classical Yang-Mills evolution, starting from adjacent *generic* random initial gauge fields in the noncompact (A, E) scheme. They calculated the KS entropy and found that the KS entropy is positive and finite even after a long time. The equilibration time scale τ_{eq} was estimated to be around 2 fm/c for $T = 350$ MeV, though with rather substantial systematic uncertainties. This result obtained by starting from a generic random initial fields shows that a significant amount of entropy is produced by the dynamical complexity inherent in the CYM equations, suggesting that thermalization in heavy-ion collisions can be at least partly achieved in the classical regime before particle production comes into play as a quantum process.

In Ref. [25], it was also observed that there are three distinct time regimes, namely a kinetic stage for short sampling times, an intermediate- and a long-time regime: i) The short sampling time is characterized by the *local Lyapunov exponents* (LLE). ii) The evolution of the distance on (long) mixing time scales is described by the usual Lyapunov exponents, which we refer to as *global Lyapunov exponents* (GLE). It is to be noted that GLEs are equivalent to the original Lyapunov exponents. iii) In the intermediate-time period, the nonlinear coupling between different field modes is significant but the energy remains localized among the primary unstable modes. The Lyapunov exponents characterizing the exponential growth of the separation of trajectories in this intermediate time period are called *intermediate Lyapunov exponents* (ILEs). We emphasize that the ILEs are the most relevant Lyapunov exponents for the thermalization of the glasma, because they characterize the time-evolution of the strongly excited Yang-Mills fields in the early stage when the field configuration is still far away from equilibrium and a quasi-classical description of the dynamics of the Yang-Mills field is appropriate.

D. Scope of this Work

In this paper, we extend the analysis done in [25] and explore the thermalization process starting from more realistic initial conditions than those adopted in Ref. [25], namely glasma-like initial conditions. We analyze the time-evolution of the distance between two trajectories starting from two adjacent points in phase space and also extract the spectrum of Lyapunov exponents from the time evolution of these fields. As was mentioned before,

we can determine whether and how early entropy production is achieved by examining the number and magnitude of the positive Lyapunov exponents. In this study, we use two glasma-like initial conditions. One is called “modulated initial condition”, where the initial color-magnetic fields B_i are spatially modulated along the z and x -axes. We call the other “constant- A initial condition”. Here both the gauge potentials A_i and the chromomagnetic fields B_i are constant, but non-commuting. It turns out that the two initial conditions give similar results for entropy production with some minor differences in the time evolution once the glasma-like initial conditions are taken.

The paper is organized as follows. In Sec. II, we introduce the basic ingredients of our simulations including the initial conditions. In Sec. III, we show the numerical results for calculations starting from the modulated initial condition. From the time evolution of the distance between two trajectories which are very close to each other initially we determine the Lyapunov exponents. We also show numerical results for simulations using the constant- A initial condition in Sec. III. Section IV is devoted to a summary and concluding remarks.

II. FORMULATION OF THE PROBLEM

In this section, we first introduce the equations of motion and the formulae needed for the analysis of chaotic behavior and the entropy production. (See Ref. [25] for details.) Then we describe the glasma-like initial conditions with fluctuations as well as the parameters chosen in our simulations.

A. Classical Yang-Mills equation

In pure Yang-Mills theory in temporal gauge $A_0^a = 0$, the Hamiltonian in the noncompact (A, E) scheme takes the following form on a cubic spatial lattice

$$H = \frac{1}{2} \sum_{x,a,i} E_i^a(x)^2 + \frac{1}{4} \sum_{x,a,i,j} F_{ij}^a(x)^2, \quad (2)$$

$$F_{ij}^a(x) = \partial_i A_j^a(x) - \partial_j A_i^a(x) + \sum_{b,c} f^{abc} A_i^b(x) A_j^c(x), \quad (3)$$

where ∂_i is the central difference operator in the i -direction, $\partial_i A(x) \equiv \{A(x+\hat{i}) - A(x-\hat{i})\}/2$, and f^{abc} are structure constants. In this study, we deal with SU(2) gauge theory, i.e., $f^{abc} = \epsilon^{abc}$, where ϵ^{abc} is the Levi-Civita tensor defined with $\epsilon^{123} = 1$. Note that all quantities in the equations are dimensionless, i.e. scaled with appropriate powers of the lattice constant.

From Eqs. (2) and (3), we get the classical equations

of motion (EOM) for $(A_i^a(x), E_i^a(x))$

$$\dot{A}_i^a(x) = E_i^a(x), \quad (4)$$

$$\dot{E}_i^a(x) = \sum_j \partial_j F_{ji}^a(x) + \sum_{b,c,j} f^{abc} A_j^b(x) F_{ji}^c(x), \quad (5)$$

which we solve with glasma-like initial conditions to be specified later. A fourth-order Runge-Kutta method is adopted to solve these EOM. It should be noted that we chose the initial condition such that it satisfies Gauss' law $(\sum_i D_i E^i(x))^a = \sum_i \partial_i E^{ia}(x) + \sum_{i,c,b} f^{acb} A_i^c E^{ib}(x) = 0$ and check its validity carefully at every time slice. Energy conservation is also checked for each time step.

B. Distance between two trajectories

A natural indicator for the chaotic behavior of the system is the “distance” between two trajectories which start from slightly different initial points in phase space. With $(A_i^a(t, \vec{r}), E_i^a(t, \vec{r}))$ being the trajectory starting from an initial point $(A_i^a(0, \vec{r}), E_i^a(0, \vec{r}))$ in phase space, we consider a second trajectory $(A_i'^a(t, \vec{r}), E_i'^a(t, \vec{r}))$ starting from an adjacent point. Then we define the distance D_{EE} (D_{FF}) between the electric fields (the field strengths) by

$$D_{EE} = \sqrt{\sum_x \left\{ \sum_{a,i} E_i^a(x)^2 - \sum_{a,i} E_i'^a(x)^2 \right\}^2}, \quad (6)$$

$$D_{FF} = \sqrt{\sum_x \left\{ \sum_{a,i,j} F_{ij}^a(x)^2 - \sum_{a,i,j} F_{ij}'^a(x)^2 \right\}^2}, \quad (7)$$

respectively. Here $F_{ij}'^a(x)$ is the field strength tensor evolved from the initial point $(A_i'^a(t=0, \vec{r}), E_i'^a(t=0, \vec{r}))$. These distances are gauge invariant under the residual gauge transformation of the EOM, namely, $E \rightarrow \Omega(\vec{x})E$ and $F \rightarrow \Omega(\vec{x})F$, where $\Omega(\vec{x})$ is a function of gauge transformations in the adjoint representation which are independent of time.

The Lyapunov exponents are extracted from the time-dependence of these distances, as is described in the next subsection.

C. Lyapunov exponents

For the two trajectories $(A_i^a(t, \vec{x}), E_i^a(t, \vec{x}))$, and $(A_i'^a(t, \vec{x}), E_i'^a(t, \vec{x}))$ the tangent vector

$$\delta X(t) = (\delta A_i^a(t, \vec{x}), \delta E_i^a(t, \vec{x}))^T \quad (8)$$

satisfies the following EOM[25],

$$\delta \dot{X}(t) = \begin{pmatrix} \mathbf{0} & \mathbf{1} \\ -H_{AA}(t) & \mathbf{0} \end{pmatrix} \delta X(t) \equiv \mathcal{H}(t) \delta X(t), \quad (9)$$

where we have introduced a matrix defined by

$$(H_{AA}(t))_{iax,jby} = \delta^2 H / \delta A_i^a(\vec{x}, t) \delta A_j^b(\vec{y}, t). \quad (10)$$

We call the matrix \mathcal{H} Hessian, and the eigenvalues of \mathcal{H} for each time slice are referred to as the local Lyapunov exponents (LLEs)[25]: As it stands, the LLE plays the role of a “temporally local” Lyapunov exponent, which specifies the departure rate of two trajectories in a short time period.

For a system where stable and unstable modes couple with each other as in the present case, an LLE does not generally agree with the Lyapunov exponent in a long time period. As an adequate way to characterize the exponential growth of the fluctuation, the authors in Ref. [25] introduced another kind of Lyapunov exponent λ^{ILE} called the intermediate Lyapunov exponent (ILE), which is an “averaged Lyapunov exponent” for an intermediate time period Δt ; i.e., a time period which is sufficiently small compared to the thermalization time but large enough to sample a significant fraction of phase space.

The explicit definition of a λ^{ILE} goes as follows: We first note that Eq. (9) is solved for any time period Δt by

$$\delta X(t + \Delta t) = U(t, t + \Delta t) \delta X(t), \quad (11)$$

$$U(t, t + \Delta t) = \mathcal{T} \left[\exp \left(\int_t^{t+\Delta t} \mathcal{H}(t + t') dt' \right) \right], \quad (12)$$

with \mathcal{T} denoting the time ordered product. The following Trotter formula for the time-evolution operator U is found convenient for a numerical evaluation;

$$\begin{aligned} U(t, t + \Delta t) &= \mathcal{T} \prod_{k=1, N} U(t_{k-1}, t_k) \\ &\simeq \mathcal{T} \prod_{k=1, N} [1 + \mathcal{H}(t_{k-1}) \delta t], \end{aligned} \quad (13)$$

where $\delta t \equiv \Delta t / N$. Diagonalizing the matrix U , we reach the definition of the ILEs

$$U_D(t, t + \Delta t) = \text{diag}(e^{\lambda_1^{\text{ILE}} \Delta t}, e^{\lambda_2^{\text{ILE}} \Delta t}, \dots). \quad (14)$$

In this study, λ^{ILE} ’s are calculated by setting $t = 0$,

$$U_D(0, \Delta t) = \text{diag}(e^{\lambda_1^{\text{ILE}} \Delta t}, e^{\lambda_2^{\text{ILE}} \Delta t}, \dots). \quad (15)$$

As the thus defined ILEs depend on the time period Δt , we examine the Δt dependence of the ILE spectrum in our later discussion.

Two comments are in order, here: A Lyapunov exponent can be (real) positive, negative, zero or purely imaginary. Liouville’s theorem tells us that the determinant of the time evolution matrix U is unity, implying that the sum of all positive and negative ILEs is zero. The KS entropy is given as a sum of positive Lyapunov exponents. The second comment concerns gauge invariance of the Lyapunov exponents. The discussion in the paper is centered on the time evolution of KS entropy which is the sum of the positive Lyapunov exponents in CYM. However, if the modes related to LLE and ILE are gauge non-invariant, the observed chaoticity does not necessarily have a physical meaning. In the Appendix we show, however, that LLE and ILE are indeed gauge invariant under time-independent gauge transformations in the temporal gauge.

Our goal is to clarify how the entropy grows during the time interval when the gauge field configuration is still far from equilibrium but has already sampled a significant fraction of phase space. Thus the KS entropy of interest should be defined as the sum of positive ILEs,

$$\frac{dS}{dt} = S_{KS} = \sum_{\lambda_i^{\text{ILE}} > 0} \lambda_i^{\text{ILE}}. \quad (16)$$

TABLE I: Parameter set for the modulated initial conditions. The column “Parameter set” gives the names of the parameter sets and the figures for which a parameter set was used.

Parameter set	lattice size	w (range of fluctuations)	ϵ_1	ϵ_2	n	m	ϵ (energy density)
M-F4 (Fig.1(a))	4^3	7.1×10^{-2}	0	0	-	-	7.15×10^{-3}
M-B4 (Fig.1(b))	4^3	0	9.7×10^{-2}	10^{-4}	3	3	7.13×10^{-3}
M-Bf4-1 (Fig.1(c) and 4)	4^3	10^{-4}	9.7×10^{-2}	10^{-4}	3	3	7.13×10^{-3}
M-f4 (Fig.1(c'))	4^3	10^{-4}	0	0	-	-	1.379×10^{-8}
M-Bf4-2 (Fig.5)	4^3	10^{-4}	6.859×10^{-2}	10^{-4}	3	3	3.529×10^{-3}
M-Bf8 (Fig.6)	8^3	10^{-4}	9.7×10^{-2}	10^{-4}	3	3	3.528×10^{-3}

D. Choice of initial conditions

As mentioned in the Introduction, realistic initial conditions for high-energy heavy-ion collisions are based on

the gauge field configuration created in the collision be-

TABLE II: Parameter set for constant A initial conditions.

Parameter set	lattice size w (width of fluctuations)	magnetic field B	ϵ (energy density)
C-Bf4 (Fig.3 and 8)	4^3	5×10^{-4}	0.15
C-Bf8 (Fig.9)	8^3	5×10^{-4}	0.15

tween two color-glass condensates, in which both the chromomagnetic and chromoelectric fields are parallel to the collision axis. These gauge field configurations serve as the starting point of the glasma.

For “modulated initial conditions” (denoted by “M-” in the names of the parameter set), the spatial components of the gauge fields are given by an oscillating background field plus small fluctuations

$$A_i^a(\vec{r}) = \delta_{i2} \left[\epsilon_1 \sin\left(\frac{2x\pi}{N_x}\right) + \epsilon_2 \sin\left(\frac{2nx\pi}{N_x}\right) \sin\left(\frac{2mz\pi}{N_z}\right) \right] + \eta_i^a(\vec{r}), \quad (17)$$

$$E_i^a(\vec{r}) = 0. \quad (18)$$

Here $\eta_i^a(\vec{r})$ is a random number that has indices for color a and spatial direction i ($i = 1, 2, 3$).

$\eta_i^a(\vec{r})$ is a uniformly distributed random number ranging from $-w$ to w , where w is the amplitude of the noise. The superscript a denotes an adjoint color index ($a = 1, \dots, (N_c^2 - 1)$). In the present study, we study $SU(N_c = 2)$. $N_x(N_z)$ is the lattice size in $x(z)$ direction. Recall that we use the temporal gauge and hence $A_0 = 0$. The parameters for the modulated initial condition are summarized in Table I. We also include initial conditions with fluctuations only (i.e. without background field), namely M-F4 and M-f4, for comparison.

When $\eta_i^a(\vec{r}) = 0$, the initial magnetic fields are written as

$$B_x^a = \partial_y A_z^a - \partial_z A_y^a + g\epsilon^{abc} A_y^b A_z^c = -\partial_z A_y^a \quad (19)$$

$$= -2m \frac{\pi}{N_z} \epsilon_2 \sin\left(\frac{2nx\pi}{N_x}\right) \cos\left(\frac{2mz\pi}{N_z}\right), \quad (20)$$

$$B_y^a = \partial_z A_x^a - \partial_x A_z^a + g\epsilon^{abc} A_y^b A_z^c = 0, \quad (21)$$

$$B_z^a = \partial_x A_y^a - \partial_y A_x^a + g\epsilon^{abc} A_y^b A_x^c = \partial_x A_y^a \quad (22)$$

$$= \frac{2\pi}{N_x} \epsilon_1 \cos\left(\frac{2x\pi}{N_x}\right) + \frac{2n\pi}{N_x} \epsilon_2 \cos\left(\frac{2nx\pi}{N_x}\right) \sin\left(\frac{2mz\pi}{N_z}\right). \quad (23)$$

Therefore, the background magnetic fields have x and z components, and are modulated along the x and z direction.

The other initial condition adopted here is the “constant- A initial condition” (denoted by “C-” in the names of parameter sets), where constant gauge fields are used to produce constant magnetic fields (see [26]),

$$A_i^a(\vec{r}) = (\delta_{i2}\delta^{a3} + \delta_{i3}\delta^{a2})\sqrt{B/g}, \quad (24)$$

$$E_i^a(\vec{r}) = 0, \quad (25)$$

where g is the coupling constant. The vector potential gives the following magnetic field configuration in $SU(2)$,

$$B_z^1 = -F_{yx}^1 = g\epsilon^{1bc} A_y^b A_x^c = g(A_y^2 A_x^3 - A_y^3 A_x^2) = -B, \quad (26)$$

where the other components of the magnetic field are zero. Since g is an irrelevant parameter in CYM, we set $g = 1$ throughout the paper. The parameters for the constant- A initial condition are summarized in Table II.

The constant- A initial condition gives a constant chromomagnetic field in one direction, and can be regarded as the simplest modeling of the initial glasma. The ϵ_1 -dominant case of the modulated initial condition ($\epsilon_1 \gg \epsilon_2$) also simulates the initial condition of the glasma with an additional amplitude oscillation in the x direction: The color-magnetic field aligns almost in the z direction, and a small longitudinal oscillation of the background field is introduced by the small value of ϵ_2 . These features of the modulated initial conditions are advantageous for the investigation of Nielsen-Olesen instabilities [12]. In a strong color-magnetic field, the modulation in the color magnetic field direction is most unstable [13, 14].

While the color-electric field is absent in the present initial conditions, the non-linear coupling between the chromo-magnetic fields and fluctuations will generate chromo-electric fields very fast. It would, of course, be desirable to incorporate chromo-electric fields in the initial condition for a more comprehensive analysis of thermalization. However, this is technically more involved and beyond the scope of the present work, because one would have to make sure that the initial condition satisfies Gauss’ law for zero color charge.

III. CHAOTICITY WITH GLASMA-LIKE INITIAL CONDITIONS

A. Time evolution of D_{EE} and D_{FF}

Here, we show the time evolution of the distances between two trajectories stemming from two adjacent points: The parameter sets used for these analyses are summarized in Tables I and II. Figures 1(a), (b), (c) and (c’) show D_{EE} and D_{FF} as functions of time for several different initial conditions, M-F4, M-B4, M-Bf4-1 and M-f4 in Table I, respectively. The two (adjacent) starting points are related to each other by

$$A_i^{\prime a}(t=0, \vec{r}) = 1.005 A_i^a(t=0, \vec{r}), \quad (27)$$

$$E_i^{\prime a}(t=0, \vec{r}) = 1.005 E_i^a(t=0, \vec{r}). \quad (28)$$

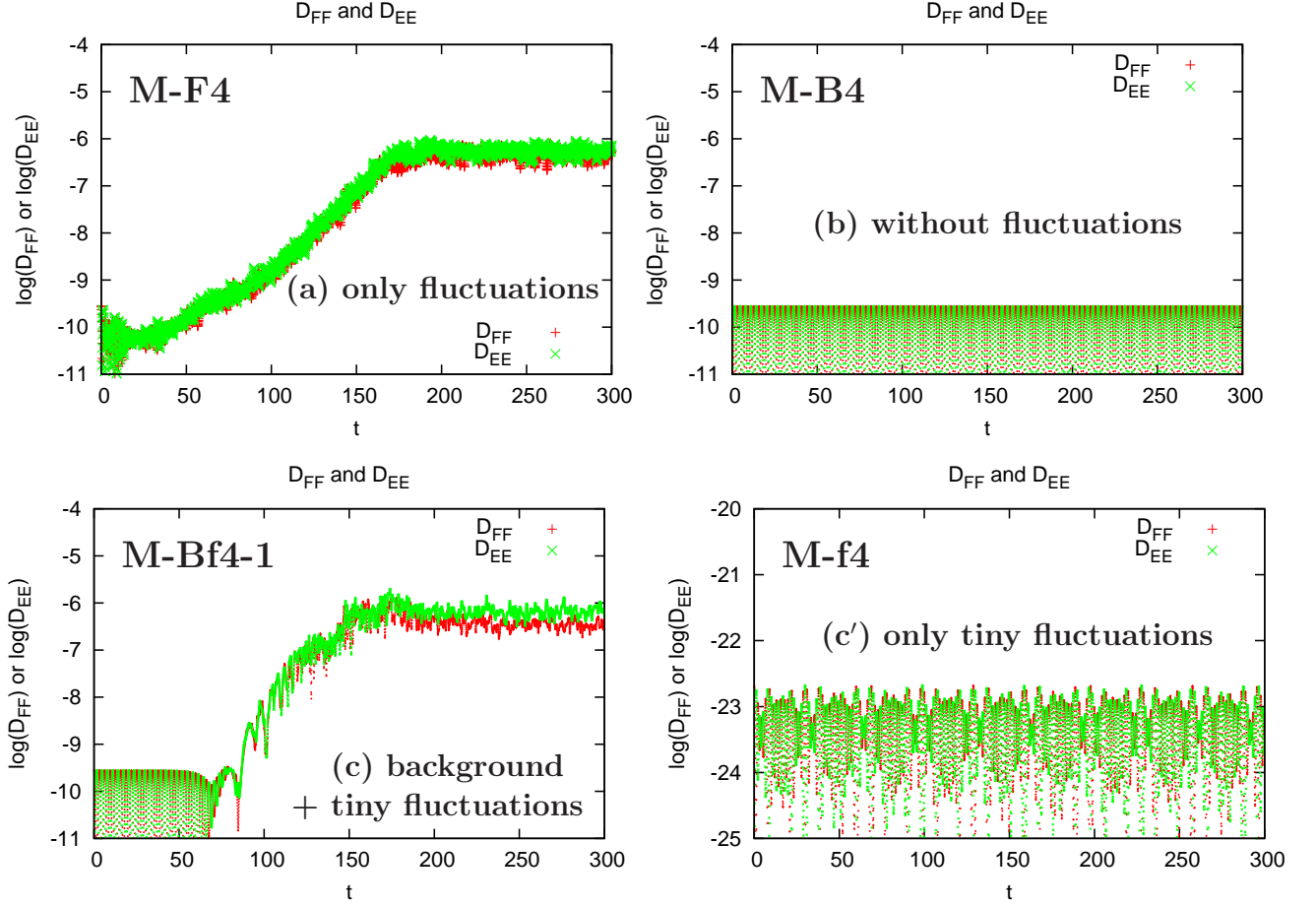


FIG. 1: Time evolution of D_{EE} and D_{FF} with the initial conditions of (a) only fluctuations (parameter set M-F4 in Table I), (b) only background field (no fluctuations, M-B4), (c) background plus tiny fluctuations (M-Bf4-1), (c') only tiny fluctuations whose amplitude is the same as that of (c) (M-f4).

We note that a linear increase in the semi-logarithmic plots shows an exponential growth of the distance, which implies an exponential sensitivity of the trajectories to the initial value. This is a typical behavior showing the chaoticity of the system, which leads to entropy production when combined with Husimi coarse-graining. The initial energy densities in the present cases are approximately the same except for the case shown in Fig. 1(c').

In Fig. 1(a), we show the time-evolution of the distances D_{EE} and D_{FF} with the initial condition M-F4, where the initial field is given by the fluctuation with no background magnetic field. We can see the exponential growth of D_{EE} and D_{FF} from $t = 30$, which shows the chaoticity of the system. After a time around $t = 170$, these distances become saturated. We find almost the same saturation times for D_{EE} and D_{FF} . This saturation property is understood to be due to the fixed total energy.

When the background magnetic fields are present in z -direction but the fluctuation is absent in the initial condition (M-B4), the exponential growth of the distances

does not manifest itself, and they only show a stationary oscillating behavior as shown in Fig.1(b). In this case, thermalization is not expected to occur.

Figure 1(c) shows the time-evolution of D_{EE} and D_{FF} with the background magnetic field plus very tiny fluctuations in the initial condition (M-Bf4-1). These D 's show an oscillatory behavior in the very early stage, then they start to grow exponentially at a certain time. In this setup, the onset time of the exponential growth is about $t = 50$.

These results suggest that the solution of CYM solely with glasma-like background field at initial time is unstable, but the instability is triggered only when tiny but finite fluctuations are imposed on top of the background field at initial time. Figure 1(c') is the numerical result solely with the initial fluctuations whose amplitude is the same as that in Fig. 1(c). We can see that the distances do not show increasing behavior at least until $t = 300$. Addition of such a tiny fluctuation is essential for the exponential growth when it couples with the glasma-like background field in the initial time, as seen in

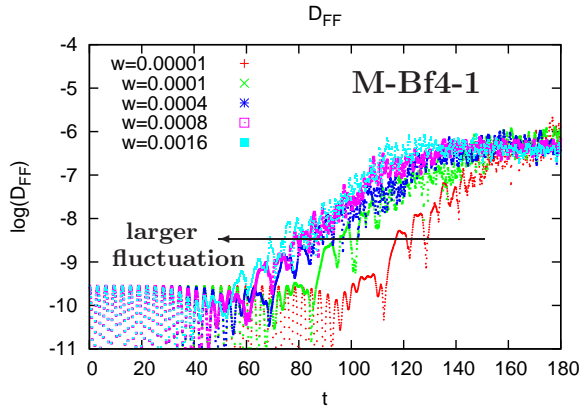


FIG. 2: Dependence of D_{EE} and D_{FF} to the various size of amplitude of fluctuations, w , from modulated initial condition (M-Bf4-1).

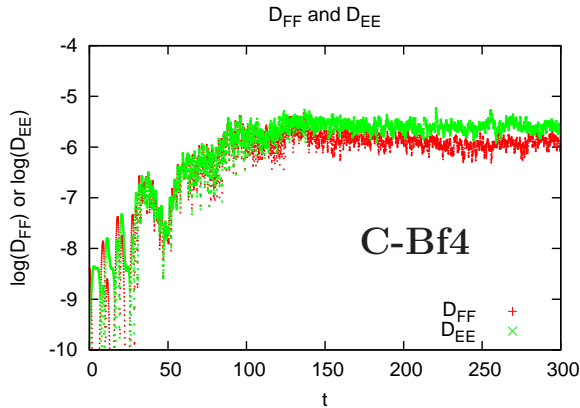


FIG. 3: Time evolution of D_{EE} and D_{FF} from the initial condition C-Bf4 where the initial background color-magnetic field is constant (C-Bf4).

Fig. 1(c). This shows that the exponential growth of the distance between two CYM solutions seen in Fig. 1(c) is not caused by the fluctuations themselves, but it is an inherent instability of the background field that is only triggered by the fluctuations.

We show the dependence of D_{FF} on the ratio of the fluctuations to the glasma-like background field in Fig. 2: The larger the relative strength of the fluctuations, the earlier the onset time of the exponential growth and the saturation time of D_{FF} . This result is of phenomenological importance, because we can predict the thermalization time once the ratio of fluctuation to the background field is known.

Figure 3 shows D_{FF} and D_{EE} for a constant A initial condition (C-Bf4). We see that both the distances grow with more pronounced oscillations of a larger amplitude than in the initial stage for the modulated initial condition, but then again become saturated and almost

constant on a time scale similar to that observed for the modulated initial condition (see Fig. 1(c)).

The oscillatory behavior in the initial stage can be understood by a linearized analysis of the CYM system, which shows that the leading-order time dependence is given by a Jacobi elliptic function [26].

The increase of the distances for these different initial conditions indicates that chaotic behavior occurs irrespective of the details of the chosen initial conditions, as long as they have some (tiny) random fluctuations on some coherent background field.

B. Time evolution of the Lyapunov spectrum

As mentioned before, the KS entropy is defined as the sum of all positive Lyapunov exponents and gives the entropy production rate. Therefore, the spectrum of Lyapunov exponents in the late stage is of paramount importance for entropy production in a CYM system. We further expect that the sum of positive intermediate Lyapunov exponents (ILEs) corresponds to the entropy production rate at a certain time. If this is the case, the time evolution of the spectrum of ILEs describes the time evolution of the thermalization process. Below we report our numerical results for the time evolution of the spectrum of positive ILEs.

Modulated initial condition

Figure 4 shows the time evolution of the spectrum of ILEs for the parameter set M-Bf4-1 in Table I. The vertical axis is the magnitude of the positive real ILEs and the horizontal axis is the label of the ILEs in descending order. Imaginary ILEs are plotted as zeros in these figures. The time slices for which the different spectra were obtained are shown in the upper right-hand corner of the figures.

The figures show that the spectrum has a step-like shape at $t = 0$, which implies the existence of degenerated, unstable, exponentially growing modes from the very beginning of the evolution. More importantly, the number of the positive Lyapunov exponents is a finite fraction of the total number of degrees of freedom. This behavior actually could be expected, because the ILE's at $t = 0$ coincide with the local Lyapunov exponents (LLEs) defined as the eigenvalues of the Hessian, and thus the existence of positive ILE's at $t = 0$ should reflect that of the unstable modes revealed in linear response theory [13].

The number of positive ILEs or unstable modes on the 4^3 lattice is around 60 at $t = 0$ and increases with time, while the magnitudes of the largest ILEs decrease during the time period of $0 < t \lesssim 100$. From a comparison with Fig. 1(c), we find that the exponential growth of the D 's starts well after the spread of the spectrum of unstable modes. This observation suggests that a nonlinear analysis including mode-mode coupling is necessary for the investigation of entropy production. The spectrum

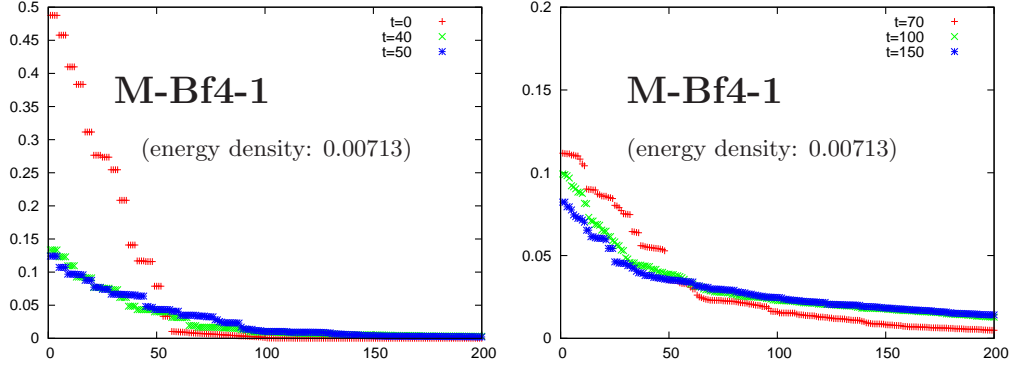


FIG. 4: Time evolution of ILE for the “modulated initial condition” with M-Bf4-1 in Table I ($V = 4^3$).

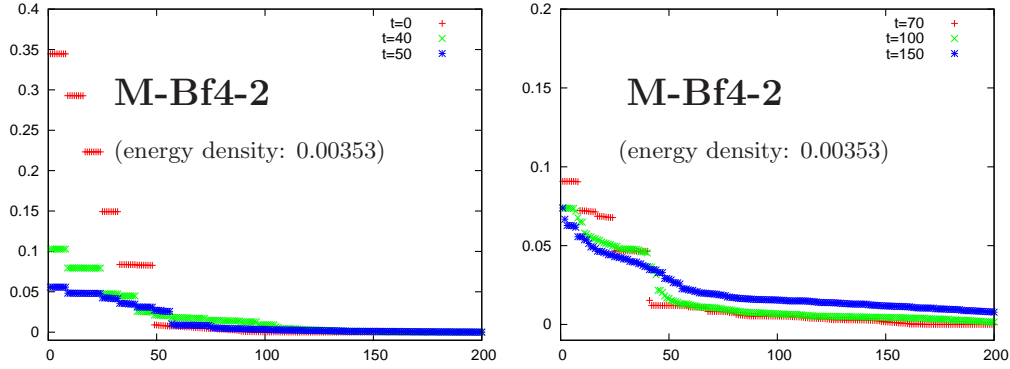


FIG. 5: Time evolution of ILE for the “modulated initial condition” with M-Bf4-2 in Table I ($V = 4^3$).

at saturation contains a finite number of positive ILEs. In fact, the number of positive ILE’s now exceeds 200, which constitutes a *macroscopic* number, comparable to the total number of modes, 1152. We conclude that the KS entropy is definitely nonzero and that entropy production is a sustained property of the glasma in CYM.

Figure 5 shows the time evolution of the spectrum of ILEs for the parameter set M-Bf4-2, where the initial energy density is about half of that for M-Bf4-1. The feature of the spectrum is the same as that for M-Bf4-1: the step-like shape at the initial time and the time dependence of the ILE spectrum. A difference is that the magnitude is smaller than for M-Bf4-1 at any point along the horizontal axis. This fact shows that KS entropy is larger for a larger energy density. We will show the value of the KS entropy in Table III.

Figure 6 shows the evolution of the ILE spectrum in a larger (8^3) volume, with the parameter set M-Bf8 shown in Table I. The plot style is the same as in Fig. 4. The spectrum again starts from a somewhat discontinuous and step-like shape at $t = 0$ and then becomes a smooth shape quite similar to that found on the smaller (4^3) lattice. The transition between the two regimes occurs at $t \simeq 50$. It should be noted that the total number of degrees of freedom, $18N^3$ for a N^3 lattice, is quite different

for the two lattices. Again, the Lyapunov spectrum becomes stable after $t \simeq 100$, containing a large number of positive ILE’s, approximately 4500, which constitutes a macroscopic fraction of the total number of degrees of freedom, which is 9216. The similarity with the results for the smaller lattice extends to quantitative details. For example, the value of the largest ILE is near 0.08 for both lattices, and the values of the ILEs for the 17% most unstable modes exceed 0.01 in both cases.

In Fig. 7, the ILE spectra for M-Bf4-2 and M-Bf8 are compared at late time, $t = 150$, where the spectrum is approximately stable. We can see that the magnitude of the ILEs for the 8^3 lattice is always larger than for 4^3 at any point along the horizontal axis. In addition, the spectra coincide for large values on the horizontal axis. Based on this analysis of volume-dependence, we expect that the ILE spectrum stays finite in infinite volume.

In Table III, the time dependence of the KS entropy divided by volume, $s_{KS} \equiv S_{KS}/V = \sum_{\lambda_i > 0} \lambda_i/V$, is shown for each initial condition, M-Bf4-1, M-Bf4-2, and M-Bf8. Note that M-Bf4-2 and M-Bf8 have the same initial energy density. For the initial condition M-Bf4-1, the value of $s_{KS} \equiv S_{KS}/V$ is about 0.23 at the initial time, drops slowly with time and finally settles around 0.12 at $t \simeq 100$. Thus, the KS entropy is surely positive

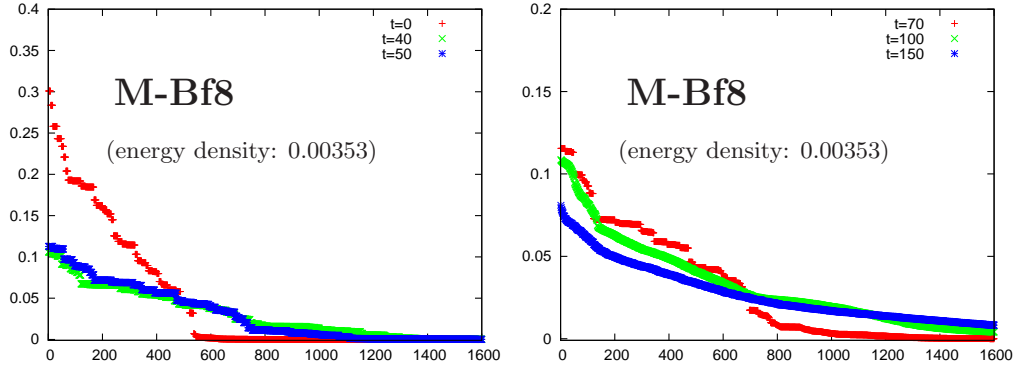


FIG. 6: Time evolution of ILE for the same initial condition as in Fig. 5 except for the lattice size (8^3 in this figure). The parameter set used in the calculation is M-Bf8 in Table I.

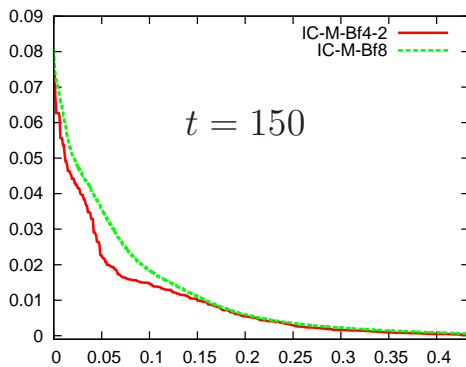


FIG. 7: Dependence of ILE spectrum on lattice size. The spectrum is plotted against the label of the ILEs divided by the total number of modes in descending order of ILE. The red-solid line shows the spectrum on the 4^3 lattice with the initial condition M-Bf4-2, and the green-dotted line shows that on the 8^3 lattice with the initial condition M-Bf8. These two initial conditions have the same energy density.

definite even at late times, implying that the entropy is produced. A similar behavior is obtained for the initial condition M-Bf4-2 which has an energy density about half of that of M-Bf4-1; s_{KS} starts from a value around 0.15, and the stable final value around 0.08 is reached at $t \simeq 150$. The larger the energy density, the larger the value of the KS entropy. In the previous study, Ref. [25], the authors found that s_{KS} scales as the fourth root of energy density, $\epsilon^{1/4}$, for random initial magnetic fields. For the initial conditions M-Bf4-1 and M-Bf4-2, the ratio of KS entropy, $0.122/0.079 \simeq 1.54$, is not so close to the fourth root of the ratio of the energy density ϵ , $(0.00706/0.00353)^{1/4} \simeq 1.19$. As the setting in this case is not isotropic, it is not clear that all dimensioned parameters should simply scale with powers of $\epsilon^{1/4}$. It could also be that the volume studied here (4^3) is insufficient for a reliable scaling analysis.

For the larger volume, M-Bf8, s_{KS} is about 0.14 at initial time and about 0.10 at $t = 150$. s_{KS} surely survives in a larger volume, and entropy production in the infinite-volume limit can be expected.

Constant- A initial condition

We show the time evolution of the ILE spectra obtained from the constant- A initial conditions with tiny fluctuation on 4^3 and 8^3 lattices in Figs. 8 and 9, respectively. At $t = 0$, the spectra have the step-like structure similar to that from the modulated initial condition, except for the detailed structures. At later time, this discontinuity of the structure disappears and the spectrum becomes smooth. After about $t = 100$, the spectrum becomes stable, and again the fraction of positive ILEs is finite. The behavior on the 8^3 lattice is quantitatively quite similar to that on the 4^3 lattice, when the horizontal axis is rescaled by the total number of modes.

Comparison of the two cases we have studied, modulated and constant- A initial conditions, which are chosen to mimic the glasma initial condition, reveals that the ILE spectra at late times are quite similar: Except for a few modes that remain very unstable ($\lambda > 0.1$) in the case of the constant- A initial condition, the largest ILE's take values around 0.08, and the modes at the 17th percentile of all modes (the 200th and 1600th modes for the 4^3 and 8^3 lattices, respectively) have ILEs around 0.01. In both cases also a much larger fraction of all modes becomes unstable at late times than in the initial phase of the evolution. The agreement suggests that entropy production occurs in the CYM dynamics for any glasma-like initial condition and that a large part of the entropy production is caused by the chaoticity of the gauge field dynamics manifested after some time, rather than by the instability of the specific gauge field configuration in the initial stage.

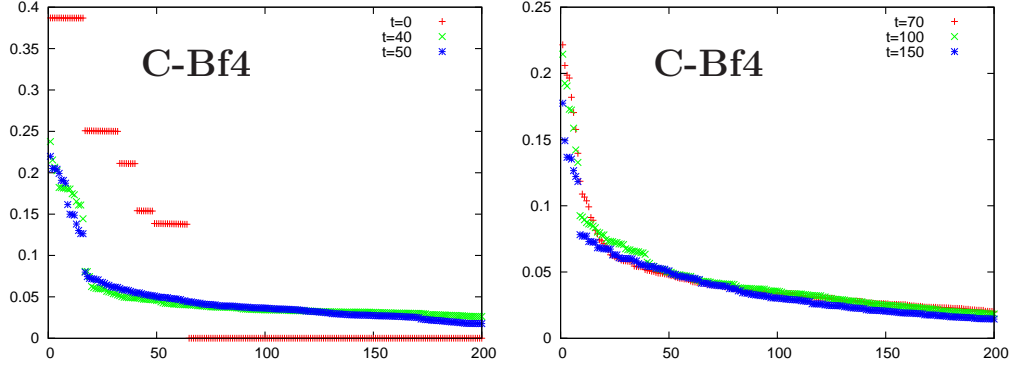


FIG. 8: Time evolution of the intermediate Lyapunov exponent spectrum for the “constant A initial condition” on the $V = 4^3$ lattice. The parameter set used in the calculation is C-Bf4 from Table II.

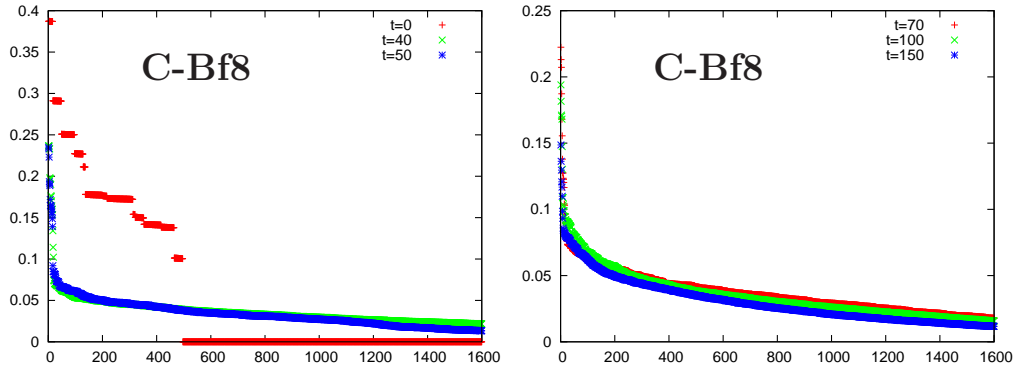


FIG. 9: Time evolution of intermediate Lyapunov exponent spectrum for the “constant A initial condition” on the $V = 8^3$ lattice. The parameter set used in the calculation is C-Bf8 from Table II.

$s_{KS} \equiv S_{KS}/V$			
	M-Bf4-1 $\epsilon = 7.13 \times 10^{-3}$	M-Bf4-2 $\epsilon = 3.53 \times 10^{-3}$	M-Bf8 $\epsilon = 3.53 \times 10^{-3}$
$t=0$	0.226	0.151	0.140
40	0.088	0.063	0.095
50	0.094	0.042	0.096
70	0.098	0.052	0.092
100	0.119	0.054	0.106
150	0.122	0.079	0.099

TABLE III: Time dependence of Kolmogorov-Sinai entropy divided by volume for initial conditions, M-Bf4-1, M-Bf4-2 and M-Bf8. ϵ denotes the energy density.

IV. SUMMARY AND CONCLUDING REMARKS

We have studied the thermalization process of classical Yang-Mills fields starting from semi-realistic glasma-like initial conditions characteristic for relativistic heavy-ion collisions. We focused on the chaotic behavior and

entropy production of the classical field theory. For this purpose we determined all Lyapunov exponents for the theory discretized on a cubic spatial point lattice. The sum of all positive Lyapunov exponents, i.e. the Kolmogorov-Sinai entropy, gives the rate of entropy production.

We considered two types of glasma-like initial conditions. One is the “modulated initial condition”, where initial chromomagnetic fields B_i^a are spatially modulated along the z and x axes. In the absence of fluctuations, this field configuration is color-independent. The other initial condition is the “constant- A initial condition”, where the gauge potentials A_i^a and chromo-magnetic fields B_i^a are both constant, but color-dependent, and only the z -component of the chromomagnetic field in one color direction is nonzero. For both types of initial conditions we added small random fluctuations to describe the noise present in the glasma fields due to the quantum fluctuations in the two colliding nuclei.

We have found that when the gauge field is given by the modulated initial condition without any fluctuations, the distance between two trajectories starting from adjacent points shows oscillatory behavior and exponential

growth is absent. When small fluctuations are present on top of the background field, the initial oscillatory behavior of the distance terminates after a short time and the exponential growth of the distance becomes robustly visible. The onset time of exponential growth depends on the ratio of the amplitude of the fluctuation to the strength of the chromomagnetic field. The fact that we do not see any exponential growth in the absence of initial fluctuations demonstrates that our numeric treatment introduces no fluctuations of relevant size.

For the modulated initial condition with small fluctuations positive Lyapunov exponents are present from the beginning. This is a reflection of the unstable modes revealed in the linear response analysis of glasma fields. We found that the number of modes with positive Lyapunov exponents increases substantially during time evolution, and that the Lyapunov spectrum reaches a stable shape when a macroscopic fraction of the modes has positive Lyapunov exponents. This implies that a bulk number of field modes contributes to the KS entropy and that the entropy production rate per unit volume is non-zero in CYM.

The dependence of the Lyapunov spectrum on the size of the spatial volume is found to be weak if the mode number is rescaled by the total number of modes, which suggests that extensive entropy production occurs in the infinite volume limit in CYM as first found by Bolte *et al.* [27].

The chaotic behavior of CYM with the noisy “constant- A initial condition” is similar to that observed for the modulated initial condition with some modifications during the initial phase of the time evolution. After an initial increase of the distance accompanied with some oscillatory behavior, the distance shows an exponential growth, and the time evolution of the spectrum of ILEs shows a qualitatively similar behavior as that seen for the modulated initial condition. The number of positive Lyapunov exponents is again found to be large, corresponding to many unstable *bulk* modes, and the entropy production rate grows approximately linear with volume also for the constant A initial condition.

The important conclusion to be drawn from our present analysis is that entropy production occurs in a robust way *at the classical field level* starting from semi-realistic initial conditions. While the classical field description of the glasma becomes invalid when thermal equilibrium is approached, the pre-equilibrium dynamics of the glasma can be simulated by classical gauge field equations, which allows to estimate the thermalization time. We therefore focused our study on the intermediate time regime, where the ILEs characterize the dynamical instability of the gauge field. Our study suggests that the magnitude of the delay time before the start of linear entropy growth depends substantially on the chosen initial condition while the entropy growth rate itself is affected at most mildly. Substantially more systematic studies are needed to decide whether there exist realistic scenarios for which the thermalization time is as small as

1 fm/c, which is the value advocated by the comparison of hydrodynamical simulations with heavy ion data.

As the gauge field approaches equilibrium and quantum effects become important by providing a physical cut-off to the ultraviolet divergences of the classical thermal field theory, the evolution of the glasma can be described by viscous hydrodynamics. It is an interesting question whether the two effective theories of the dynamics of an equilibrating quark-gluon plasma can be directly joined or whether there is a need for an additional formalism interpolating between these two regimes.

ACKNOWLEDGMENTS

The calculations were performed mainly by using the NEC-SX9 at Osaka University. This work was supported in part by Grant-in-Aid for Scientific Research from the Japan Society for the Promotion of Science (JSPS) and the Ministry of Education, Culture, Sports, Science and Technology of Japan (MEXT) (Nos. 20540265, Innovative Areas (No. 2004: 23105713, and No. 2404: 24105001, 24105008), 23340067, 24340054, 24540271), by the Yukawa International Program for Quark-Hadron Sciences, by a Grant-in-Aid for the global COE program “The Next Generation of Physics, Spun from Universality and Emergence” from MEXT and by BMBF (06RY7195).

Appendix : Proof of the gauge invariance of Lyapunov spectra

We here show that the local/intermediate Lyapunov exponents are gauge invariant under the remaining gauge transformations in temporal gauge, i.e., time-independent gauge transformations. The Hessian $\mathcal{H}(t)$ in a concrete expression is

$$\mathcal{H}(t) = \begin{pmatrix} \mathbf{0} & \mathbf{1} \\ -H_{AA}(t) & \mathbf{0} \end{pmatrix}, \quad (1)$$

where $(H_{AA}(t))_{iax,jby} \equiv \delta^2 H / \delta A_i^a(\vec{x}, t) \delta A_j^b(\vec{y}, t)$ is a second derivative in terms of gauge fields. Gauge fields A_i^a are transformed according to $A_i^a(\vec{x}, t) = (\Omega(\vec{x}) A_i(\vec{x}, t))^a + W_i^a(\vec{x}, t)$, with a time-independent orthogonal matrix $\Omega(\vec{x})$, i.e., $\Omega(\vec{x}) \Omega^T(\vec{x}) = \mathbf{1}$. $W_i^a(\vec{x}, t)$ is a possible term independent of gauge fields.

Paying attention to the chain rule,

$$\frac{\delta}{\delta A_i^a(\vec{x}, t)} = \frac{\delta}{\delta A_i^b(\vec{x}, t)} \frac{\delta A_i^b(\vec{x}, t)}{\delta A_i^a(\vec{x}, t)} = \frac{\delta}{\delta A_i^b(\vec{x}, t)} (\Omega^T(\vec{x}))_{ba}$$

the transformation property of H_{AA} for a time-independent gauge transformation $\Omega(\vec{x})$ in the adjoint

representation of $SU(N)$ is found to be

$$\begin{aligned} H_{AA}(t) &= \delta^2 H / \delta A_i^a(\vec{x}, t) \delta A_j^b(\vec{y}, t) \\ \rightarrow H'_{AA}(t) &= \delta H^2 / \delta A_i^a(\vec{x}, t) \delta A_j^b(\vec{y}, t) \\ &= (\Omega H_{AA}(t) \Omega^T)_{iax, jby}. \end{aligned} \quad (2)$$

(Note that the Hamiltonian H is gauge invariant.) Defining an orthogonal matrix

$$\bar{\Omega}(\vec{x}) \equiv \begin{pmatrix} \Omega(\vec{x}) & \mathbf{0} \\ \mathbf{0} & \Omega(\vec{x}) \end{pmatrix}, \quad (3)$$

the gauge transformation of $\mathcal{H}(t)$ can be expressed as

$$\mathcal{H}(t) \rightarrow \mathcal{H}'(t) = \bar{\Omega} \mathcal{H}(t) \bar{\Omega}^T \quad (4)$$

in a similar manner. Taking orthogonality and time-independence of $\bar{\Omega}(\vec{x})$ into account, the local and intermediate Lyapunov spectra of the Hessian $\mathcal{H}(t)$ are easily

shown to be gauge invariant. In fact, a time-ordered product of the Hessian

$$U(t, t + \Delta t) = \mathcal{T} \left[\exp \left(\int_t^{t+\Delta t} \mathcal{H}(t + t') dt' \right) \right] \quad (5)$$

transforms as

$$\begin{aligned} U(t, t + \Delta t) &\rightarrow U'(t, t + \Delta t) \\ &= \mathcal{T} \left[\exp \left(\int_t^{t+\Delta t} \bar{\Omega} \mathcal{H}(t + t') \bar{\Omega}^T dt' \right) \right] \\ &= \bar{\Omega} \mathcal{T} \left[\exp \left(\int_t^{t+\Delta t} \mathcal{H}(t + t') dt' \right) \right] \bar{\Omega}^T \\ &= \bar{\Omega} U(t, t + \Delta t) \bar{\Omega}^T, \end{aligned} \quad (6)$$

and gives the same (gauge invariant) intermediate Lyapunov spectra.

-
- [1] U. Heinz, private communication; R. Chatterjee and D. K. Srivastava, Nucl. Phys. A **830**, 579C (2009).
 - [2] U.W.Heinz and P.F.Kolb, Nucl.Phys.A**702**, 269 (2002) [arXiv:hep-ph/0111075].
 - [3] R. Baier, A. H. Mueller, D. Schiff and D. T. Son, Phys. Lett. B **502**, 51 (2001) [hep-ph/0009237].
 - [4] B. H. Alver, C. Gombeaud, M. Luzum and J. -Y. Ollitrault, Phys. Rev. C **82**, 034913 (2010) [arXiv:1007.5469 [nucl-th]].
 - [5] H. Petersen, G. -Y. Qin, S. A. Bass and B. Müller, Phys. Rev. C **82**, 041901 (2010) [arXiv:1008.0625 [nucl-th]].
 - [6] A. Dumitru and Y. Nara, Phys. Rev. C **85**, 034907 (2012) [arXiv:1201.6382 [nucl-th]].
 - [7] K. Dusling, T. Epelbaum, F. Gelis and R. Venugopalan, arXiv:1210.6053 [hep-ph].
 - [8] For reviews: E. Iancu, A. Leonidov and L. McLerran, arXiv:hep-ph/0202270; E. Iancu and R. Venugopalan, arXiv:hep-ph/0303204; F. Gelis, T. Lappi and R. Venugopalan, Int. J. Mod. Phys. E**16**, 2595 (2007).
 - [9] L. McLerran and R. Venugopalan, Phys. Rev. D**49**, 2233 (1994); *ibid.* **49** 3552 (1994); *ibid.* **50**, 2225 (1994).
 - [10] E. S. Weibel, Phys. Rev. Lett. **2**, 83 (1959).
 - [11] S. Mrówczyński, Phys. Lett. B **314**, 118 (1993).
 - [12] N. K. Nielsen and P. Olesen, Nucl. Phys. B **144**, 376 (1978).
 - [13] H. Fujii and K. Itakura, Nucl. Phys. A**809**, 88 (2008).
 - [14] H. Fujii, K. Itakura, and A. Iwazaki, Nucl. Phys. A**828**, 178 (2009).
 - [15] A. Dumitru, Y. Nara and M. Strickland, Phys. Rev. D **75**, 025016 (2007) [arXiv:hep-ph/0604149].
 - [16] T. Lappi and L. McLerran, Nucl. Phys. A **772**, 200 (2006) [hep-ph/0602189].
 - [17] T. Kunihiro, B. Müller, A. Ohnishi and A. Schäfer, Prog. Theor. Phys. **121**, 555 (2009) [arXiv:0809.4831 [hep-ph]].
 - [18] A. Wehrl, Rev. Mod. Phys. **50**, 221 (1978).
 - [19] K. Husimi, Proc. Phys. Math. Soc. Jpn. **22**, 246 (1940).
 - [20] For a review of results before 1995 see: T. S. Biró, S. G. Matinyan and B. Müller, *Chaos and gauge field theory*, World Sci. Lect. Notes Phys. **56**, 1 (1994).
 - [21] S. G. Matinyan, E. B. Prokhorenko and G. K. Savvidy, JETP Lett. **44**, 138 (1986); Nucl. Phys. B **298**, 414 (1988).
 - [22] B. Müller and A. Trajanov, Phys. Rev. Lett. **68**, 3387 (1992).
 - [23] T. S. Biró, C. Gong and B. Müller, Phys. Rev. D **52**, 1260 (1995) [arXiv:hep-ph/9409392].
 - [24] C. Gong, Phys. Rev. D **49**, 2642 (1994) [arXiv:hep-lat/9308001].
 - [25] T. Kunihiro, B. Müller, A. Ohnishi, A. Schäfer, T. T. Takahashi and A. Yamamoto, Phys. Rev. D **82**, 114015 (2010).
 - [26] J. Berges, S. Scheffler, S. Schlichting and D. Sexty, Phys. Rev. D **85**, 034507 (2012) [arXiv:1111.2751 [hep-ph]].
 - [27] J. Bolte, B. Müller and A. Schäfer, Phys. Rev. D **61**, 054506 (2000) [arXiv:hep-lat/9906037].